Received: 10 April 2022 | Revised: 6 December 2022 | Accepted: 13 December 2022

DOI: 10.1111/geb.13632

Global Ecology and Biogeography | A Journal of Macroecology | WILEY

RESEARCH ARTICLE

Disentangling thermal from alternative drivers of reflectance in jewel beetles: A macroecological study

Lu-Yi Wang[1] | Amanda M. Franklin[1] | Andrew F. Hugall[1,2] | Iliana Medina[1] | Devi Stuart-Fox[1]

[1]School of Biosciences, The University of Melbourne, Melbourne, Victoria, Australia

[2]Sciences Department, Museums Victoria, Melbourne, Victoria, Australia

Correspondence
Lu-Yi Wang, School of Biosciences, The University of Melbourne, Parkville, Melbourne, VIC 3052, Australia.
Email: luyiwangtw@gmail.com

Funding information
Australian Research Council, Grant/Award Number: DP190102203 and FT180100216

Handling Editor: Andrew Rominger

Abstract

Aim: To predict future colour–climate relationships, it is important to distinguish thermal drivers of reflectance from other evolutionary drivers. We aimed to achieve this by comparing relationships between climate and coloration in ultraviolet–visible (UV–Vis) and near-infrared (NIR) light, separately.

Location: Samples were distributed primarily across Australia and North America, with some from Africa and Asia.

Major taxa studied: Coleoptera: Buprestidae.

Methods: We used jewel beetles as models to identify climatic drivers of reflectance, because jewel beetles have highly diverse coloration and a wide distribution and are often active in hot conditions. Specifically, we tested the association between climate, body size and reflectance using a phylogenetic comparative analysis for three wavebands (UV–Vis, NIR and total).

Results: Reflectance of jewel beetles was more strongly predicted by body size than by climate. NIR reflectance and total reflectance were not associated with climate, but larger beetles had higher NIR reflectance. For UV–Vis reflectance, small beetles were darker in warmer and more humid environments, whereas there was no association with climate for large beetles.

Main conclusions: Our study suggests that variation in reflectance of jewel beetles is not driven by thermal requirements and highlights the importance of considering NIR reflectance when evaluating explanations of the effects of colour on thermoregulation.

KEYWORDS
Bogert's rule, coloration, global warming, Gloger's rule, melanin, near-infrared, thermoregulation

1 | INTRODUCTION

With growing concerns about global warming, how animals adapt to a warming climate has become a time-critical question. Animal coloration is a key functional trait, and its evolutionary trajectory in response to warming climates is a topic of current interest and debate (Delhey et al., 2020; Tian & Benton, 2020a, 2020b). The response of animal coloration to warming climates depends on whether current

colour–climate relationships are driven by selection for thermal benefits or for other functions of coloration [e.g., camouflage, protection from ultraviolet (UV) damage]. Variation in animal coloration along climate gradients has been generalized into several ecogeographical rules, such as Bogert's rule and Gloger's rule, which are likely to arise from different ecological and evolutionary drivers. Bogert's rule (or thermal melanism hypothesis) predicts that ectotherms tend to be darker in colder regions, possibly to increase heating rate and radiative heat gain (Bogert, 1949; Clusella-Trullas et al., 2007). In contrast, Gloger's rule, originally described for endotherms but also extending to ectotherms, describes a trend for darker coloration in more humid environments (Delhey, 2019; Rensch, 1929). This pattern is likely to be attributable to the non-thermal functions of melanin, such as protection from UV damage, abrasion or pathogens (Delhey, 2019; True, 2003). The patterns described by these ecogeographical rules are not mutually exclusive and depend on the climatic variation and life history of particular animal groups. Therefore, to understand current and projected colour–climate relationships, it is essential to distinguish selection for thermal control from other drivers, and to do so for animal groups with a range of climatic distributions and life histories.

One way to determine whether macroecological patterns of animal coloration are generated by selection for thermal benefits is to consider solar radiation in wavelengths beyond visible colour. The full spectrum of sunlight comprises ultraviolet–visible wavelengths (UV–Vis; 300–700 nm) and near-infrared wavelengths (NIR; 700–2500 nm). Approximately half of the energy in direct sunlight falls in each of these two wavebands, meaning that both contribute to heat gain, proportional to the reflectance or absorbance of the integument (i.e., percentage reflectance or absorbance). However, given that NIR wavelengths cannot be perceived visually by most terrestrial animals, reflectance in these wavelengths is likely to be selected primarily for thermal needs (Stuart-Fox et al., 2017), whereas visible reflectance will be influenced by selection for other functions of colour, such as communication or camouflage. Consequently, if selection for thermal benefits drives macroecological colour–climate relationships, we expect a correlation between temperature-related climate variables and total solar reflectance (UV–Vis–NIR), and particularly NIR reflectance. Recent studies that have considered NIR wavelengths have detected such correlations, supporting selection for thermal benefits (Kang et al., 2021; Medina et al., 2018; Munro et al., 2019). However, current evidence is restricted to Australian birds (Medina et al., 2018) and Australian and European butterflies (Kang et al., 2021; Munro et al., 2019). It is difficult to generalize these results to other groups, especially for insects that vary greatly in life history, habitat and behaviour.

Insects are poikilotherms whose body temperatures are greatly influenced by environmental conditions. Hence, solar energy might play a more important role for insects than for endotherms, such as mammals and birds (Gates, 1980a). Beetles are one of the most successful and colourful groups of animals on Earth, but are poorly represented in macroevolutionary and macroecological studies, possibly owing to a lack of phylogenetic information. Jewel beetles (Coleoptera: Buprestidae) are a group of insects with diverse visible colours and are likely also to have variable NIR reflectance (Wang et al., 2021). The adults are diurnal and active during the warmest seasons and spend most of their time on host plants, feeding and finding potential mates (Hawkeswood, 1978, 1981a, 1981b). Our recent study on jewel beetles shows that the heating rate of isolated elytra decreased by .011°C min^{-1} for every 1% increase in NIR reflectivity under illumination equivalent to <.5 solar intensity, controlling for effects of convection and conduction (Wang et al., 2021). In contrast, we found no significant effect of UV–Vis reflectivity, because variation in UV–Vis reflectivity among the sampled species was much less than the variation in NIR reflectivity. This suggests the potential importance of climate in shaping reflectance, especially for NIR wavelengths. A comprehensive investigation into jewel beetles is required to understand how much the effect of NIR reflectance on heat transfer in a finely controlled setting is linked to macroevolutionary pattern.

Here, we aimed to identify whether climate variables drive variation in reflectance of jewel beetles. Specifically, we tested the association between climate and reflectance in different wavelength ranges (UV–Vis, NIR and total) within a phylogenetic framework. Initially, we measured the reflectance of the beetle samples from calibrated photographs in the three wavebands. Next, we ran three separate phylogenetic comparative analyses on the reflectance for each waveband to test what climate components best predict the reflectance. Additionally, we included body size in the analysis, because size has been reported to affect thermoregulation in many animals, including jewel beetles (Peralta-Maraver & Rezende, 2021; Stevenson, 1985a; Wang et al., 2021). If reflectance is important for thermoregulation, in hotter climates we expect higher NIR reflectance (independent of UV–Vis reflectance) and total reflectance, which accounts for the overall heat gain of an organism. Given that UV–Vis reflectance could be under numerous, sometimes conflicting, selective pressures, we expect it to show a weaker correlation with climate and, possibly, to be associated with humidity, as predicted by Gloger's rule. It is also unclear how different colour-producing mechanisms (pigment and/or structures) correspond to NIR reflectance. For example, Shawkey et al. (2017) showed that iridescent structurally coloured feathers in sunbirds have lower NIR reflectance than pigmented feathers. Therefore, we also investigated whether structural beetle colours have lower NIR reflectance than colours produced by other probable mechanisms.

2 | MATERIALS AND METHODS

2.1 | Specimen sampling

Jewel beetle specimens were sampled from the Australian National Insect Collection (ANIC). Species were selected based on the phylogeny provided by Evans et al. (2015). We sampled the same species from the phylogeny if these species were available in the ANIC; otherwise, we chose a representative of the same genus,

tribe or subfamily. If more than one representative of a genus, tribe or subfamily was available to choose from, we selected the species that had different visible coloration from the beetles already selected, in order to increase colour diversity in our samples. We ensured that all subfamilies were well represented, except for the subfamily Galbellinae, which is a small and rare subfamily and not present in ANIC collections. For each species, we sampled two to four specimens (mode = 3) depending on the availability in the collection. In addition to ANIC specimens, we included 12 locally collected *Castiarina* species in our dataset to expand the species and colour diversity. The local samples were collected on bushes by foliage beating from 26–27 November 2018 in Gembrook and Emerald, VIC, Australia. Before further measurements, we kept the local beetles in the laboratory until they died naturally. In total, we obtained data for 223 specimens from 81 species and 45 genera (Supporting Information Table S1).

2.2 | Specimen imaging

We took UV, visible and NIR photographs for each specimen to derive reflectance in these three wavelength ranges (details below). Capturing reflectance using a camera instead of a spectrometer coupled to an integrating sphere enabled us to measure the reflectance of small beetles or fine-scale patterns (i.e., <4 mm). The specimens were pin-mounted on a piece of grey foam and photographed individually, except for those glued on the same board. In each photograph, we included a scale bar and a 40% achromatic reflectance standard (LabSphere, North Sutton, NH, USA) for calibration.

The photographs were taken using a camera (D7200; Nikon, Tokyo, Japan) with a UV–Vis–NIR transmissive lens (60 mm Apo Macro, CoastalOpt; JenOptik, Jena, Germany). We placed different optical filters (Edmund Optics, Barrington, NJ, USA) to photograph in UV (filter model numbers: 84715, 84723 and 49095), visible (84754 and 84727) and NIR (84760 and 84735; Figure 1). The combination of the camera sensor and optical filters enabled us to capture wavelengths of 350–400 nm (range, 50 nm) for UV, 400–700 nm (range, 300 nm) for visible and 700–1000 nm (range, 300 nm) for NIR. The total wavelength range (350–1000 nm) covers *c*. 75.7% of total solar energy. For the light sources, we used a modified flash unit (Nikon SB-140 UVIR clone; BeyondVisible, USA) for UV and visible photographs and a tungsten halogen lamp (150 W HT150 tube; Arlec, Melbourne, VIC, Australia) for NIR photographs (for detailed camera set-up, see Munro et al., 2019). A cylindrical diffuser was placed over the sample, scale bar and reflectance standard on the grey foam to create an even illumination. We divided the specimens into four size categories, for which we used different camera exposure settings and camera heights (Supporting Information Table S2) to obtain the optimal resolution and illumination for specimens in each size category.

2.3 | Reflectance and body size

From the photographs, we derived an estimate of reflectance in UV, visible and NIR wavelength ranges, in addition to body size. For reflectance, we focused on the elytra, because they are the major area exposed to direct sunlight. For each individual, we chose one region that was not shaded and had no glare spot as a region of interest (ROI) for each colour on the elytra (colour patch). The same ROI was selected for UV, visible and NIR photographs for the same specimen. To quantify reflectance of the ROIs, we first obtained the mean pixel intensity values for red (R), green (G) and blue (B) channels of the ROIs and the achromatic standard for

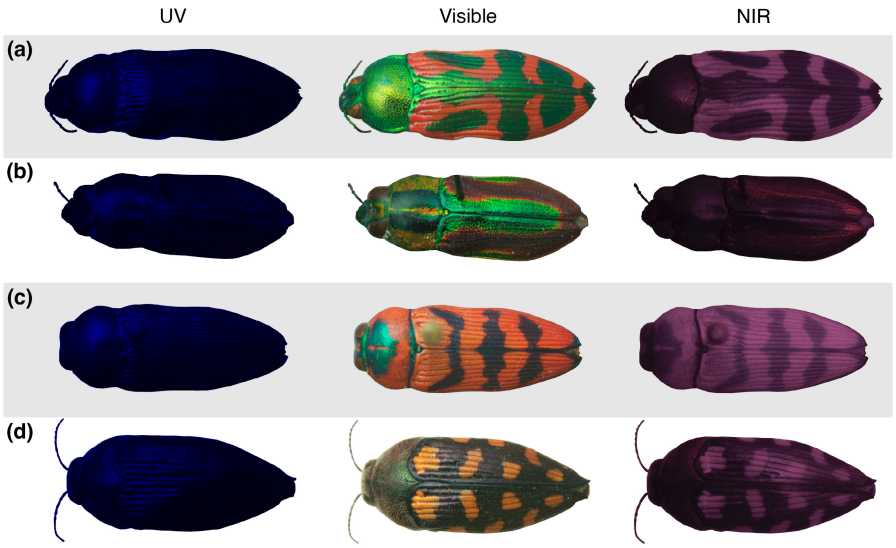

FIGURE 1 Ultraviolet (UV; left), visible (middle) and near-infrared (NIR; left) photographs of (a) *Castiarina ignota*, (b) *Selagis caloptera*, (c) *Calotemognatha varicollis* and (d) *Astraeus crassus*. Lighter colour indicates higher reflectance. Almost all beetles show little reflectance in UV wavelengths. In some beetles, the reflectance pattern varies between visible and NIR. The reflectance of different colour patches in the three wavelength ranges for all species used is in the Supporting Information (Table S5)

each photograph using the MEASURERGB plugin in IMAGEJ (v.1.52a; Schneider et al., 2012). We next calibrated the RGB values from the responses of the camera to the known achromatic standards (for calibration details, see Supporting Information Supplementary Information S1; Munro et al., 2019). From these achromatic standards, we derived an equation to estimate the reflectance for each colour channel and for camera settings of each size category. For each waveband, we selected the channels based on sensitivity of the camera sensors (sensor sensitivity data provided by Nikon under a non-disclosure agreement). For UV, we used the B channel; for visible, we used R, G and B channels; and for NIR, we used the R and B channels. When more than one channel was used, we averaged the calibrated values to give an estimate of average reflectance for each colour patch. To obtain the average reflectance of the whole beetle, we weighted the reflectance of each colour patch by the area it occupied on the elytra measured using IMAGEJ from Vis photographs. Finally, to derive UV–Vis reflectance (350–700 nm) and total reflectance (350–1000 nm), we weighted the reflectance relative to the spectral range of each waveband using Equation (1) or Equation (2), respectively:

$$R_{\mathrm{UV-Vis}} = \frac{R_{\mathrm{UV}} \times 50 + R_{\mathrm{Vis}} \times 300}{50 + 300}, \quad (1)$$

$$R_{\mathrm{total}} = \frac{R_{\mathrm{UV}} \times 50 + R_{\mathrm{Vis}} \times 300 + R_{\mathrm{NIR}} \times 300}{50 + 300 + 300}, \quad (2)$$

where R_{UV}, R_{Vis}, R_{NIR}, $R_{\mathrm{UV-Vis}}$ and R_{total} are the reflectance in the UV, visible, NIR, UV–Vis and total (UV–Vis–NIR) range, respectively.

To ensure that we captured real variation in UV–Vis and NIR wavebands from the photographs, we correlated the reflectance derived from photographs with reflectance measured using a spectrometer for a subset of 11 species (Supporting Information Supplementary Information S2).

For body size, we measured the area of an ovoid (in millimetres squared) for each specimen from Vis photographs as a proxy of the incident area using IMAGEJ.

2.4 | Climate data

We compiled climate data for each specimen locality to represent the climate variance within species. Specifically, we extracted the climate data at the global positioning system (GPS) coordinates of the museum labels or our own collection sites. If the GPS locations were not available on the specimen labels, we extracted the coordinates from naturally vegetated regions of the labelled locations on Google Maps. For three specimens, no information about the collection sites was available; therefore, we chose locations with the greatest concentration of records of the focal species from Atlas of Living Australia (ALA; https://www.ala.org.au) for Australian species or from iNaturalist (https://www.inaturalist.org) for non-Australian species.

Ambient temperature is an important factor influencing the thermoregulation strategy adopted by an animal, and humidity is the major component of Gloger's rule. Therefore, we selected nine climate variables related to temperature and humidity, namely mean temperature of the warmest quarter (in degrees Celsius), representing the active season of jewel beetles, annual mean maximum temperature (in degrees Celsius), annual mean minimum temperature (in degrees Celsius), mean diurnal temperature range (in degrees Celsius), temperature seasonality (in degrees Celsius; SD ×100), precipitation of the warmest quarter (in millimetres), precipitation seasonality (coefficient of variation), mean annual water vapour pressure (in kilopascals) and solar radiation of the warmest quarter (in kilojoules per metre squared per day). The climate data were downloaded from the WorldClim database (v.2.1; Fick & Hijmans, 2017). We used average values for the available years (1970–2000) at the spatial resolution of 2.5′ (*c.* 4.7 km). Bioclimatic variables (derivatives of monthly values) from the database were used for the annual temperature, humidity and seasonality data. For variables not available as annual values from bioclimatic variables, we downloaded the values from the monthly historical data and calculated the annual averages manually in R (i.e., annual mean maximum temperature, annual mean minimum temperature, annual water vapour pressure and solar radiation of the warmest quarter). To minimize redundancy, we excluded variables that were highly correlated with another ($r > .8$; Supporting Information Table S6). We excluded annual mean maximum temperature, which was highly correlated with mean temperature of the warmest quarter ($r = .949$), and annual mean minimum temperature, which was highly correlated with mean annual water vapour pressure ($r = .880$). Mean temperature of the warmest quarter and mean annual water vapour pressure were also highly correlated with each other ($r = .849$). In total, we included seven climate variables (mean temperature of the warmest quarter, mean diurnal temperature range, temperature seasonality, precipitation of the warmest quarter, precipitation seasonality, mean annual water vapour pressure and solar radiation of the warmest quarter) in the subsequent analysis.

Owing to the relatively large number of climate variables (seven), we took a conventional variable reduction approach (e.g., Hurtado et al., 2020; Medina et al., 2018; Miller et al., 2019). Specifically, we performed a principal components analysis (PCA) on the seven climate variables to reduce dimensionality. The climate data were scaled before the PCAs. We selected the principal components (PCs) that had eigenvalues greater than one (here, PC1 and PC2), reducing the seven original climate variables to two variables for use in subsequent phylogenetic comparative analyses.

2.5 | Phylogenetic comparative analysis

We tested whether the reflectance of the jewel beetles could be predicted by climate and body size using a phylogenetic mixed model approach. To obtain an estimate of the phylogenetic relationships between the 81 species in our dataset, we built a supermatrix tree

of Buprestidae based on two mitochondrial and three nuclear genes (6330 sites). We used genetic information available on GenBank (Benson et al., 2017), especially the data of Evans et al. (2015), with additional phylogenetic information from McKenna et al. (2019) for calibrating key outgroup and basal nodes. Taxonomy and nomenclature were based on Catelogue of Life (https://www.catalogueoflife.org), iNaturalist and Insecta.pro (http://insecta.pro); in particular, the accepted species and higher ranks of genus, tribe and subfamily.

For phylogenetic analysis, we used a supermatrix of 125 taxa comprising the desired 81 focal species plus 44 additional non-focal taxa that were included to improve model specification and phylogenetic inference (e.g., Zwickl & Hillis, 2002). Owing to patchy data, for 18 species we substituted gene sequences to create a single genus representative. Of our 81 focal taxa, 48 had no molecular data, hence they were incorporated a priori based on taxonomic affiliation, using a combination of two subfamily-, seven tribe- and 13 genus-level topological constraints (Supporting Information Table S9; Figure S3). This method is very similar to many others (e.g., Eme et al., 2019; Thomas et al., 2013) where taxa are grafted onto backbone trees within predefined lineages via a birth–death model, and is essentially the same as done by Eme et al. (2019), where this is done simultaneously with whole tree inference (i.e., by using hard topology constraints in BEAST). Further details of phylogenetic supermatrix assembly and inference are provided in the Supporting Information (Supplementary Information S3).

We sampled 1300 post-burn-in trees generated in Bayesian phylogenetic analyses (BEAST; Bouckaert et al., 2014) to account for uncertainty in node ages and topology. Non-focal species were then pruned out for the subsequent phylogenetic comparative analyses. We note the limitations of using "synthetic" phylogenies constructed using a combination of sequence data and taxonomic rank substitution (Li et al., 2019; Rabosky, 2015); however, given that the focus of this study was on trait–climate correlations, it was important to maximize the taxonomic and geographical spread of samples to enable robust conclusion. To account for additional phylogenetic uncertainty, we ran analyses on a large set of post-burn-in trees (1300 trees), providing conservative error bounds on estimates of trait–climate correlations.

We ran three separate phylogenetically controlled mixed models, one for each reflectance wavelength range (UV–Vis, NIR and total). In each model, we included the reflectance as the response variable, and the two climatic principal components (PC1 and PC2), body size, and the interactions between body size and climatic PCs as predictor variables (Figure 2). Body size was ln-transformed before being included in the models to facilitate convergence. Additionally, we set species as a random factor to account for the multiple (one to four) specimens included for each species. The UV–Vis reflectance and NIR reflectance are parts of the same continuous spectrum and are often highly correlated. Some previous studies have accounted for this correlation by taking the residuals of NIR reflectance regressed against UV–Vis (Kang et al., 2021; Munro et al., 2019). In our dataset, UV–Vis and NIR reflectance exhibited only a weak correlation (Pearson's correlation, $r = .160$, $P < .05$), meaning that residuals are not appropriate. Instead, we included UV–Vis reflectance as a covariate in the NIR model to account for the variation in UV–Vis reflectance. The models were performed at the individual level, and the intraspecific variation was much smaller than interspecific variation (Supporting Information Table S8).

All the models were run in R (v.3.6.3; R Core Team, 2018) using the MCMCglmm package (Hadfield, 2010). Following Ross et al. (2013) and Stuart-Fox et al. (2021), we ran the Markov chain Monte Carlo (MCMC) comparative analyses for 2000 iterations on the 1300 post-burn-in trees. In each iteration, the last MCMC sample was saved, and its latent variables and variance components were passed to the next iteration as starting values. We repeated this process for each of the 1300 trees and discarded the first 300 runs as burn-in. We used a weakly informative inverse Wishart prior for the covariance and parameter-expanded priors for the random effects in all models. To examine convergence, we checked the trace plots of each variable visually using the "plot" command in R and checked whether the effective sample size of each parameter was >1000 to ensure low autocorrelation. We report the significance of predictor variables in pMCMC, which is two times the posterior probability that the estimate is either negative or positive and can be interpreted as the Bayesian equivalent to the traditional *p*-value (e.g., Hadfield et al., 2013; Ross et al., 2013). We also presented the 95% credibility intervals (CIs) of the estimates from the posterior distribution for the predictor variables, which we considered biologically significant if the intervals did not include zero.

2.6 | Relationship between NIR reflectance and colour mechanism

Jewel beetles can use pigments and/or structures to produce colour, resulting in diverse optical effects in visible wavelengths. However, it is unclear how these different mechanisms are correlated with NIR reflectance. To investigate this, we examined the association between the likely mechanism of individual colour patches and the corresponding NIR reflectance of those patches. Initially, we used the visible light photographs to classify each colour patch of the jewel beetles into three coarse categories based on their likely colour production: structural, melanin pigmented and non-melanin pigmented. We defined human-visible green, blue, violet or other patches with metallic sheens as structural, human-visible black and dark brown patches as melanin pigmented, and human-visible red, yellow, orange, light brown and white patches as non-melanin pigmented. We based this classification on known mechanisms of beetle coloration (Noh et al., 2016; Seago et al., 2009). For this analysis, we included only beetle species in which the colour patches could be classified easily into the above three categories. In total, we classified 254 colour patches from 166 beetles belonging to 59 species. Among them, 53 melanin patches were from 53 beetles belonging to 18 species, 95 structural patches were from 91 beetles belonging 33 species,

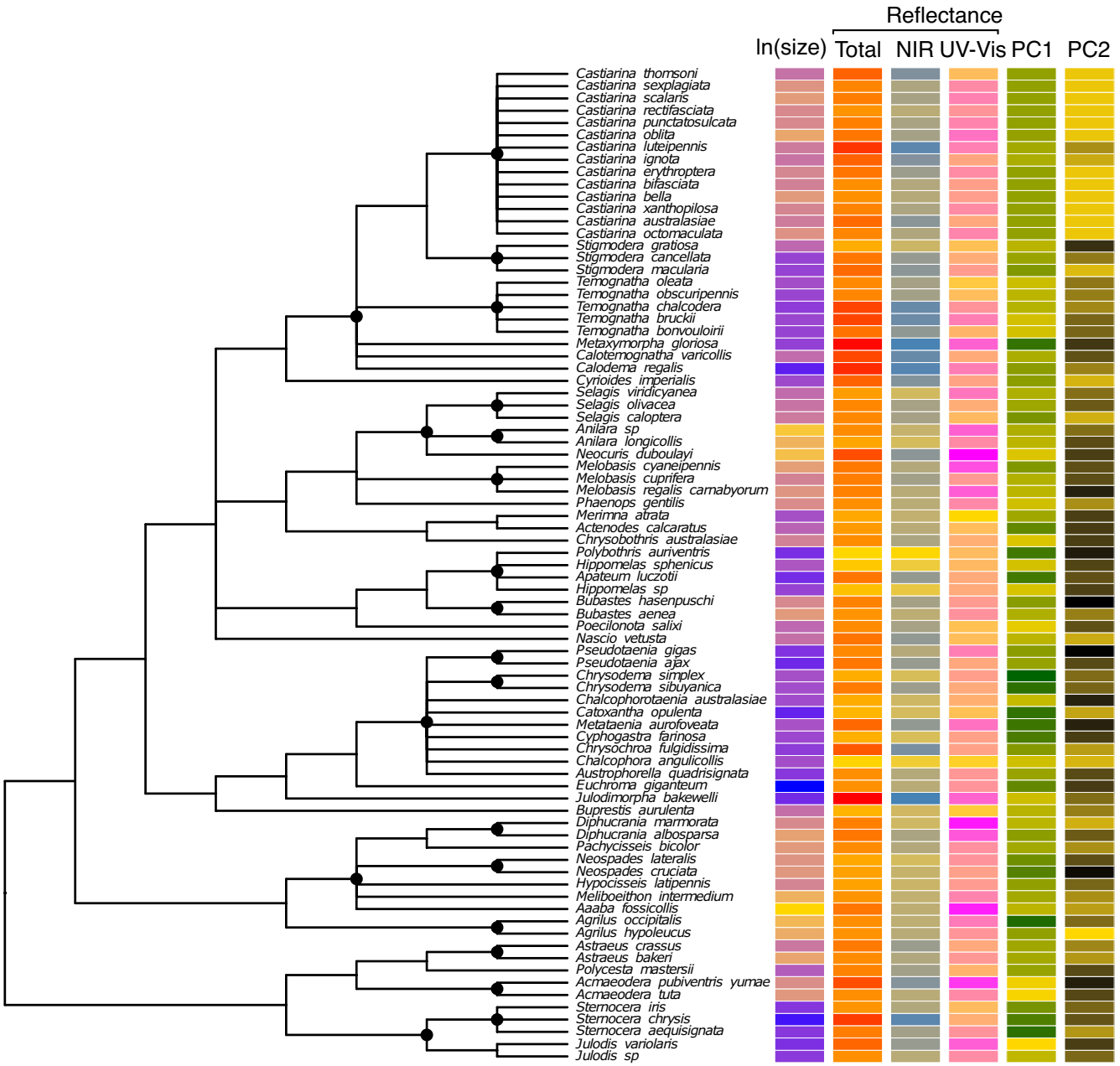

FIGURE 2 Trait and climatic variation and the phylogenetic distribution of this variation among the 81 jewel beetle species. The heatmaps show the variation in body size, reflectivity [total, near-infrared (NIR) and ultraviolet–visible (UV–Vis)] and climatic proxies (principal components PC1 and PC2; correlated with warm, humid climates and warm climates without significant wet/dry season, respectively) among species. The reflectance data were ln-transformed for visualization. The depicted phylogeny is a majority rule consensus of the 1300 tree samples used in the comparative analyses, with nodes constrained for interpolating taxa marked by black dots (see also Supporting Information Figure S3)

and 106 pigmented patches were from 97 beetles belonging to 33 species.

We ran an MCMCGLMM model within a phylogenetic framework, with NIR reflectance of a given colour patch as the response variable and the UV–Vis reflectance of the same patch, mechanism and their interaction as predictor variables. To account for multiple individuals per species and multiple colour patches per individual, we set species and individual as random factors. We used the same methodology and model parameters as for the climate models described above. We did not correlate colour mechanism with climate, because individual colour patches, which vary among species in both their presence and relative size, do not correspond to the total reflectance of a beetle. Additionally, given that only 18 species had melanic colour patches, the sample size was too small to identify meaningful correlations between the presence of melanic patches and climate at this broad scale of analysis.

3 | RESULTS

3.1 | Climate principal components

Climate PC1 and climate PC2 explained 51.4% and 29.6% of total climate variation, respectively. Climate PC1 loaded most strongly and positively against precipitation of the warmest quarter and mean annual water vapour pressure, and negatively against mean diurnal temperature range, temperature seasonality and solar radiation of the warmest quarter (Supporting Information Table S7). High climate PC1 values represented warm, humid environments with moderate daily and seasonal temperature fluctuations, characteristic of tropical forested environments, whereas low climate PC1 values represented climates with hot, dry summers and cool winters, characteristic of mediterranean climates (Figure 3). Climate PC2 loaded most strongly and positively against mean temperature of the warmest quarter and precipitation seasonality (Supporting Information Table S7). Higher climate PC2 values represented warm climates without significant wet/dry season, characteristic of tropical rain forested environments and/or hot desert climates, whereas lower climate PC2 values represented cold climates with seasonal rainfall, characteristic of temperate oceanic climates (Supporting Information Figure S2).

3.2 | Evolutionary association between reflectance, body size and climate

UV–Vis reflectance was predicted by an interaction between body size and climate PC1. Smaller beetles tended to be darker (lower UV–Vis reflectance) in warmer and more humid environments (Figure 4a; Table 1; Supporting Information Figures S4 and S5), whereas there was no relationship between climate and UV–Vis reflectance for larger beetles (Table 1). PC2 and its interaction with size had no correlation with UV–Vis reflectance either (Table 1). For NIR and total reflectance, we found no evidence of correlation with climate PCs, nor with the interaction between climate PCs and body size (Table 1). NIR reflectance was positively associated with body size (Figure 4b; Table 1) and increased by 6.3% as the beetle increased one ln(body size). Total reflectance was not associated with climate PCs, body size or any of their interactions (Table 1).

3.3 | Effect of colour mechanism on reflectance

Non-melanin pigmented colour patches (e.g., red, yellow) had much higher NIR reflectance than structural and melanin pigmented colour patches when UV–Vis reflectance was controlled (Figure 5; Table 2). On average, non-melanin pigmented patches had 37.5% and 38.2% significantly higher NIR reflectance than structural and melanic patches, respectively (Table 2). In contrast, structural and melanin pigmented colour patches had similar NIR reflectance (Supporting Information Table S3). There was no evidence for a correlation between UV–Vis and NIR reflectance overall or for any colour mechanism (main effect of UV–Vis, interaction terms; Table 2).

4 | DISCUSSION

In the present study, we used a global-scale dataset to identify climate drivers of UV–Vis, NIR and total reflectance in jewel beetles. We found that the reflectance of jewel beetles was more strongly predicted by body size than by climate gradients. Larger beetles had higher NIR reflectance than smaller beetles, but no climate components predicted either NIR or total reflectance. Smaller beetles in warmer and more humid climates tended to have lower UV–Vis reflectance (darker), as predicted by Gloger's rule, but there was no relationship between climate and UV–Vis reflectance for larger beetles. Combined, our results show that both NIR reflectance and UV–Vis reflectance of jewel beetles are likely to be driven by factors other than selection for thermoregulation, which differs from the results of previous studies on birds and butterflies (Kang et al., 2021;

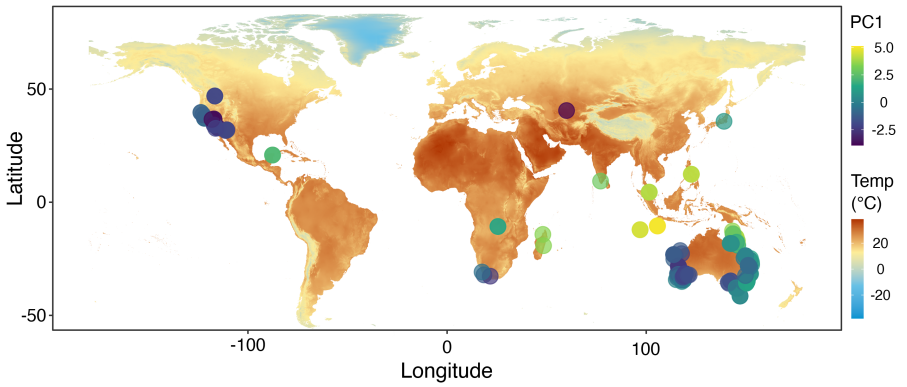

FIGURE 3 Geographical distribution of climate principal component 1 (PC1) values for each specimen at the collection coordinates (N = 223). Dot colours show the PC1 values (positively correlated with warm, humid climates), and map colours show the average temperature of the warmest quarter at the spatial resolution of 2.5′ from 1970 to 2000 [obtained from WorldClim (v.2.1); Fick & Hijmans, 2017]

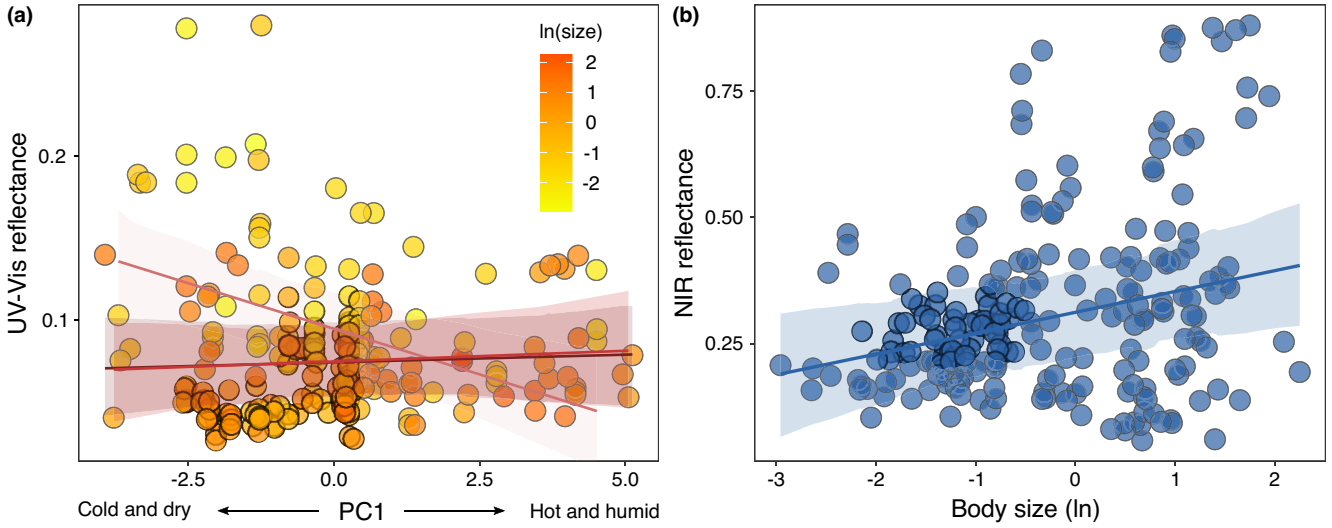

FIGURE 4 Associations between (a) principal component 1 (PC1) and ultraviolet–visible (UV–Vis) reflectance and (b) body size and near-infrared (NIR) reflectance. Regression lines and 95% confidence intervals in (a) and (b) were obtained from simplified Markov chain Monte Carlo models containing only significant variables (Table 1) conducted on the maximum clade credibility tree and are for visualization only. In (a), the light red line, the red line and the dark red line (largely overlapping with the red line) represent the regression lines for small, medium and large beetles, respectively. Patterns for insignificant variables are shown in the Supporting Information (Figure S4)

TABLE 1 Summary of the phylogenetic mixed models for total, near-infrared and ultraviolet–visible wavelengths

Range	Predictor	Posterior mean	95% Credibility interval	Effective sample size	pMCMC
Total	Intercept	.164	(.116, .207)	972.667	.001
	PC1	−.004	(−.011, .002)	858.287	.242
	PC2	0	(−.01, .011)	1153.611	.952
	Ln(body size)	.012	(−.006, .028)	1036.944	.138
	PC1 × ln(body size)	.002	(−.003, .007)	1000	.48
	PC2 × ln(body size)	−.004	(−.011, .003)	1000	.304
NIR	Intercept	.238	(.134, .353)	1000	.001
	PC1	−.006	(−.02, .008)	1000	.432
	PC2	−.002	(−.024, .018)	814.775	.88
	Ln(body size)	.062	**(.028, .099)**	1000	**.001**
	UV–Vis reflectance	1.009	**(.534, 1.452)**	810.598	**.001**
	PC1 × ln(body size)	−.004	(−.015, .006)	1000	.48
	PC2 × ln(body size)	−.014	(−.028, .003)	1000	.086
UV–Vis	intercept	.077	(.053, .098)	1000	.001
	PC1	−.002	(−.006, .002)	1000	.278
	PC2	.003	(−.003, .009)	1000	.29
	Ln(body size)	−.015	**(−.023, −.007)**	1000	**.001**
	PC1 × ln(body size)	.004	**(.001, .007)**	1000	**.004**
	PC2 × ln(body size)	.002	(−.003, .006)	1000	.454

Note: The predictor is highlighted in bold when pMCMC < .05. A plot of the distribution of estimates across the 1000 trees is given in the Supporting Information (Figure S5). pMCMC is two times the posterior probability that the estimate is either negative or positive (whichever is the smallest) and the value can be interpreted as a Bayesian equivalent to the traditional *p*-value.
Abbreviations: NIR, near-infrared; PC, principal component; UV–Vis, ultraviolet–visible.

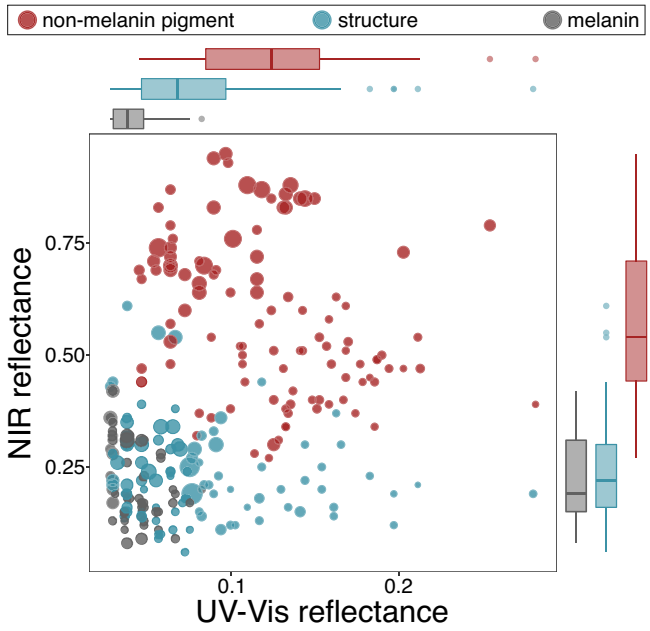

FIGURE 5 The association between ultraviolet–visible (UV–Vis) and near-infrared (NIR) reflectance for melanic (black), non-melanic pigment (red) and structural (blue) colour patches. The box and whisker plots at the top and right sides show the reflectance distribution of colour patches in UV–Vis and NIR ranges, respectively. The figure shows 254 colour patches from a subset of 166 beetles of 59 species, with each dot representing one colour patch. Dot size represents the relative body size of the beetle, not the size of the colour patch

Medina et al., 2018; Munro et al., 2019). This difference stresses the need to examine a broader range of taxonomic groups and climates to gain a comprehensive understanding of the reflectance–climate relationship.

Our results highlight the value of taking NIR reflectance into account when linking thermoregulation to the patterns described by ecogeographical rules. By considering NIR reflectance, we could decipher whether variation in reflectance is driven by thermal requirements, because it is unlikely that the selection for thermal benefits acts only on the UV–Vis range. Without considering NIR wavelengths, we could not exclude selection for thermal benefits as a possible explanation for why small beetles were darker (lower UV–Vis reflectance) in warmer and more humid climates. However, total reflectance, which is most relevant for heat gain, was not correlated with climate. NIR reflectance (controlling for UV–Vis reflectance), which is primarily relevant for thermal functions, was also uncorrelated with climate PCs. Together, these results strongly suggest that selection for thermal benefits does not explain the correlation between UV–Vis reflectance and climate for smaller beetles. Here, we tested only the effect reflectance, accounting for body size; however, it is possible that other morphological variables, such as hair, cuticle thickness or wax coatings, contribute to thermoregulation.

Melanin is the main source of dark coloration (i.e., black and dark brown) in insects (Noh et al., 2016) and contributes to both visual and non-visual functions that might be associated with climate. Visual functions of melanin, such as signalling or camouflage, might relate to the habitat of the animal. For example, darker butterflies are better camouflaged and experience lower predation in shady tropical forests (Cheng et al., 2018). Likewise, it is possible that darker coloration improves camouflage for small jewel beetles in tropical habitats. Melanin also has several non-visual functions, including thermoregulation, UV protection, desiccation tolerance, pathogen resistance and abrasion resistance (Dubovskiy et al., 2013; True, 2003). Pathogen infection by parasites, fungi or viruses might pose a higher risk in the tropics owing to the ideal temperature and humidity conditions for pathogen growth and reproduction. Melanic alleles are associated with pathogen resistance (Mikkola & Rantala, 2010; True, 2003), whereby darker morphs have higher resistance (e.g., Wilson et al., 2001). Jewel beetles might be darker in the tropics owing to a higher melanin concentration that helps to protect against pathogen intrusion. According to our mechanism dataset, ~63% of the dark colour patches of small beetles (smaller than the median) were likely to be produced by melanin. In contrast, only 30% of dark colour patches of large beetles were likely to be produced by melanin. In summary, the darker coloration of small jewel beetles in the tropics might be selected for pathogen resistance or visual protection rather than the efficiency of heat absorption.

We found no association between NIR reflectance and climate, but larger beetles had higher NIR reflectance. Despite the lack of association between NIR reflectance and climate among the sampled species, we cannot completely rule out a role of NIR in thermoregulation. Larger beetles have higher NIR reflectance, which could be because higher NIR reflectance compensates for the thermal consequences of larger body size. A larger body size affects thermoregulation through greater thermal inertia, increased surface area, lower surface area-to-volume ratio and greater body height (relative to thickness of the boundary layer of the substrate surface) (Gates, 1980b; Pincebourde et al., 2021; Stevenson, 1985a, 1985b; Wang et al., 2021). It takes longer for larger insects to reach thermal equilibrium, but they can reach higher steady-state body temperatures and retain those temperatures for longer periods owing to greater thermal inertia (Stevenson, 1985a). For example, among naturally occurring insects on leaves, large insects are warmer than smaller ones (compared with leaf surface, 4–12°C higher for larger insects and <5°C higher for smaller insects; Pincebourde et al., 2021). In the same study, a manipulative field experiment using 15- versus 2-mm-diameter clay spheres of the same colour showed a similar pattern. In contrast, smaller insects both warm up and cool down faster (Stevenson, 1985a). Adult jewel beetles spend most of time foraging and finding potential mates on host plants. When sunny, they are often exposed to sunlight whilst perching on the flowers/leaves on which they feed. Their larger surface area might result in greater radiative heat absorptance than for smaller beetles (Gates, 1965; Walsberg, 1992). Having higher NIR reflectance reduces the solar radiative heat load and potentially mitigates the thermal consequences of larger body size. This could extend activity time on host plants by delaying overheating (Wang et al., 2021), with consequences for fitness. For example, *Colias* butterflies with longer

TABLE 2 Summary of the phylogenetic mixed models for the association between near-infrared and ultraviolet–visible reflectance

Predictor	Posterior mean	95% Credibility interval	Effective sample size	pMCMC
Intercept (non-melanin pigmented)	.607	(.49, .705)	1000	.001
UV–Vis reflectance	−.18	(−.625, .271)	1000	.442
Mechanism				
Non-melanin pigmented – melanin	−.385	**(−.484, −.279)**	1165.473	**.001**
Non-melanin pigmented – structural	−.375	**(−.454, −.313)**	1000	**.001**
Interaction				
UV–Vis reflectance × melanin	.966	(−.97, 3.105)	1000	.374
UV–Vis reflectance × structural	.218	(−.573, .939)	1000	.588

pMCMC is two times the posterior probability that the estimate is either negative or positive (whichever is the smallest) and the value can be interpreted as a Bayesian equivalent to the frequentist *p*-value.

Abbreviations: NIR, near-infrared; UV–Vis, ultraviolet–visible.

flight time have higher reproductive success (Ellers & Boggs, 2004; Kingsolver, 1983).

Alternatively, the observed increase in NIR reflectance with body size could be a secondary consequence of cuticle structure rather than having an adaptive function. Integument structures (e.g., spacing, size, geometry and the arrangement of the structural elements) affect optical properties in both UV–Vis and NIR wavelengths (Krishna et al., 2020; Shi et al., 2015; Teyssier et al., 2015). However, we know very little about the relationship between cuticle microstructure and NIR reflectance and whether size might influence this. The association between NIR reflectance and body size might be simply a side effect of cuticle structures correlated with body size, such as cuticle thickness, without specific selection. It is crucial to understand the interaction between cuticle microstructures and NIR light, because mechanisms might enhance or constrain NIR reflectance. Jewel beetle colours can be produced by structures alone (Durrer & Villiger, 1972; Kinoshita & Yoshioka, 2005) or in combination with pigments. Our results showed that structural colours had lower NIR reflectance compared with non-melanin pigmented colours, accounting for UV–Vis reflectance. A similar pattern has been found in sunbirds, in which the iridescent feathers (structural colour) have lower NIR reflectance than melanin and non-melanin pigmented colours (Shawkey et al., 2017). The high NIR reflectance of what we have termed "non-melanin pigmented colours" might result from the absorption spectrum of pigments or even the structural arrangement of pigment granules (Wilts et al., 2017). The difference in NIR reflectance associated with different mechanisms suggested by our analysis (albeit coarse) indicates that further investigation into mechanisms is warranted.

Relationships between reflectance, climate gradients and body size have been examined in limited taxa, namely Australian birds and butterflies and European butterflies (Kang et al., 2021; Medina et al., 2018; Munro et al., 2019). The associations between reflectance, climate and size are inconsistent between the above-mentioned studies on butterflies and also between these studies and our results. For example, the NIR reflectance of both Australian butterflies and European butterflies are correlated with warm climates but have opposite correlations between wing size and NIR reflectance, possibly owing to different thermal functions. Larger Australian butterflies have higher NIR reflectance probably to mitigate overheating, whereas larger European butterflies have lower NIR reflectance, probably to facilitate warming (Kang et al., 2021; Munro et al., 2019). In contrast, for jewel beetles, though NIR reflectance is negatively associated with size, it is not associated with climate and therefore less likely to be driven by thermal functions. Overall, correlations between climate and reflectance identified in the present and previous studies on butterflies suggest that a thermal function of reflectance might be less prominent in jewel beetles than in butterflies. This might be explained by the ecology and behaviour of these taxa. For example, jewel beetles seek shade to reduce radiative heat load and prevent overheating when it is hot and sunny. In contrast, butterflies can open or close their wings or change their orientation relative to the sun to minimize or maximize heat gain (Clench, 1966).

Taken together, our results show different evolutionary drivers for NIR and UV–Vis reflectance of the sampled jewel beetle species. Although NIR reflectance influences heat transfer in jewel beetles (Wang et al., 2021), by considering both NIR and UV–Vis reflectance our study shows that thermoregulation is not a strong driver for reflectance variation among jewel beetle species at the macroecological scale. The sampled species represent a small proportion of the *c*. 15,500 buprestid species but capture representative variation in reflectance and climatic niche among the four main subfamilies. Therefore, our data suggest that for jewel

beetles, the answer to the question whether animals will be lighter or darker in a warming climate is likely to be neither. Here, we stress the importance of considering NIR reflectance when evaluating explanations related to thermoregulation for ecogeographical rules. Additionally, we highlight the importance of broadening taxonomic groups for the study of NIR reflectance, because the evolutionary drivers are likely to differ between animals with different ecology and environments.

AUTHOR CONTRIBUTIONS

D.S.-F., L.-Y.W. and A.M.F. conceived and designed the study and analytical approaches. L.-Y.W. collected the data and drafted the manuscript. L.-Y.W. analysed the data with assistance from I.M. A.F.H. conducted the phylogenetic reconstruction. All authors contributed to interpretation, edited the manuscript and gave final approval for publication.

ACKNOWLEDGEMENTS

We thank the Australian National Insect Collection for the jewel beetle loan and Casper J. van der Kooi for the helpful comments on the manuscript. This study was supported by the Australian Research Council (grant numbers DP190102203 and FT180100216 to D.S.-F.). Open access publishing facilitated by The University of Melbourne, as part of the Wiley - The University of Melbourne agreement via the Council of Australian University Librarians.

CONFLICT OF INTEREST

The authors declare no competing interests.

DATA AVAILABILITY STATEMENT

The dataset and R code are available from Dryad Digital Repository (https://doi.org/10.5061/dryad.8w9ghx3pr).

ORCID

Lu-Yi Wang https://orcid.org/0000-0001-6980-3782
Amanda M. Franklin https://orcid.org/0000-0002-8650-8344
Iliana Medina https://orcid.org/0000-0002-1021-5035
Devi Stuart-Fox https://orcid.org/0000-0003-3362-1412

REFERENCES

Benson, D. A., Cavanaugh, M., Clark, K., Karsch-Mizrachi, I., Lipman, D. J., Ostell, J., & Sayers, E. W. (2017). GenBank. *Nucleic Acids Research*, *45*(D1), D37–D42. https://doi.org/10.1093/nar/gkw1070

Bogert, C. M. (1949). Thermoregulation in reptiles, a factor in evolution. *Evolution*, *3*(3), 195–211. https://doi.org/10.2307/2405558

Bouckaert, R., Heled, J., Kuhnert, D., Vaughan, T., Wu, C. H., Xie, D., Suchard, M. A., Rambaut, A., & Drummond, A. J. (2014). BEAST 2: A software platform for bayesian evolutionary analysis. *PLoS Computational Biology*, *10*(4), e1003537. https://doi.org/10.1371/journal.pcbi.1003537

Cheng, W., Xing, S., Chen, Y., Lin, R., Bonebrake, T. C., & Nakamura, A. (2018). Dark butterflies camouflaged from predation in dark tropical forest understories. *Ecological Entomology*, *43*(3), 304–309. https://doi.org/10.1111/een.12499

Clench, H. K. (1966). Behavioral thermoregulation in butterflies. *Ecology*, *47*(6), 1021–1034. https://doi.org/10.2307/1935649

Clusella-Trullas, S., van Wyk, J. H., & Spotila, J. R. (2007). Thermal melanism in ectotherms. *Journal of Thermal Biology*, *32*(5), 235–245. https://doi.org/10.1016/j.jtherbio.2007.01.013

Delhey, K. (2019). A review of Gloger's rule, an ecogeographical rule of colour: Definitions, interpretations and evidence. *Biological Reviews*, *94*(4), 1294–1316. https://doi.org/10.1111/brv.12503

Delhey, K., Dale, J., Valcu, M., & Kempenaers, B. (2020). Why climate change should generally lead to lighter coloured animals. *Current Biology*, *30*(23), R1406–R1407.

Dubovskiy, I. M., Whitten, M. A., Kryukov, V. Y., Yaroslavtseva, O. N., Grizanova, E. V., Greig, C., Mukherjee, K., Vilcinskas, A., Mitkovets, P. V., Glupov, V. V., & Butt, T. M. (2013). More than a colour change: Insect melanism, disease resistance and fecundity. *Proceedings of the Royal Society B: Biological Sciences*, *280*(1763), 20130584. https://doi.org/10.1098/rspb.2013.0584

Durrer, H., & Villiger, W. (1972). Schillerfarben von *Euchroma gigantea* (L.): (Coleoptera: Buprestidae): Elektronenmikroskopische untersuchung der elytra. *International Journal of Insect Morphology and Embryology*, *1*(3), 233–240. https://doi.org/10.1016/0020-7322(72)90031-1

Ellers, J., & Boggs, C. L. (2004). Functional ecological implications of intraspecific differences in wing melanization in *Colias* butterflies. *Biological Journal of the Linnean Society*, *82*(1), 79–87. https://doi.org/10.1111/j.1095-8312.2004.00319.x

Eme, D., Anderson, M. J., Struthers, C. D., Roberts, C. D., & Liggins, L. (2019). An integrated pathway for building regional phylogenies for ecological studies. *Global Ecology and Biogeography*, *28*(12), 1899–1911. https://doi.org/10.1111/geb.12986

Evans, A. M., McKenna, D. D., Bellamy, C. L., & Farrell, B. D. (2015). Large-scale molecular phylogeny of metallic wood-boring beetles (Coleoptera: Buprestoidea) provides new insights into relationships and reveals multiple evolutionary origins of the larval leaf-mining habit. *Systematic Entomology*, *40*(2), 385–400.

Fick, S. E., & Hijmans, R. J. (2017). WorldClim 2: New 1-km spatial resolution climate surfaces for global land areas. *International Journal of Climatology*, *37*(12), 4302–4315. https://doi.org/10.1002/joc.5086

Gates, D. M. (1965). Radiant energy, its receipt and disposal. In P. E. Waggoner, D. M. Gates, E. K. Webb, W. R. van Wijk, J. A. Businger, T. V. Crawford, C. H. Hendershott, D. N. Moss, H. D. Johnson, W. S. Chepil, W. R. Henson, W. R. Gardner, B. Slavík, C. W. Thornthwaite, F. K. Hare, & J. D. McQuigg (Eds.), *Agricultural meteorology* (pp. 1–26). American Meteorological Society.

Gates, D. M. (1980a). Energy budgets of animals. In D. E. Reichle (Ed.), *Biophysical ecology* (pp. 382–462). Springer New York.

Gates, D. M. (1980b). Longwave and Total radiation. In D. E. Reichle (Ed.), *Biophysical ecology* (pp. 148–180). Springer New York.

Hadfield, J. D. (2010). MCMC methods for multi-response generalized linear mixed models: The MCMCglmm R package. *Journal of Statistical Software*, *33*(2), 1–22. https://doi.org/10.18637/jss.v033.i02

Hadfield, J. D., Heap, E. A., Bayer, F., Mittell, E. A., & Crouch, N. M. A. (2013). Disentangling genetic and prenatal sources of familial resemblance across ontogeny in a wild passerine. *Evolution*, *67*(9), 2701–2713. https://doi.org/10.1111/evo.12144

Hawkeswood, T. (1978). Observations on some Buprestidae (Coleoptera) from the Blue Mountains, N.S.W. *Australian Zoologist*, *19*(3), 257–275.

Hawkeswood, T. (1981a). Observations on some jewel beetles (Coleoptera Buprestidae) from the Armidale district, North-Eastern New South Wales. *Victorian Naturalist*, *98*, 152–155.

Hawkeswood, T. (1981b). Observations on two sympatric species of Buprestidae (Coleoptera) from sand dunes on the north coast of New South Wales. *Victorian Naturalist*, *98*, 146–151.

Hurtado, P., Prieto, M., Martinez-Vilalta, J., Giordani, P., Aragon, G., Lopez-Angulo, J., Košuthová, A., Merinero, S., Díaz-Peña, E. M., Rosas, T., Benesperi, R., Bianchi, E., Grube, M., Mayrhofer, H., Nascimbene, J., Wedin, M., Westberg, M., & Martinez, I. (2020).

Disentangling functional trait variation and covariation in epiphytic lichens along a continent-wide latitudinal gradient. *Proceedings of the Royal Society B: Biological Sciences*, *287*(1922), 20192862. https://doi.org/10.1098/rspb.2019.2862

Kang, C., Im, S., Lee, W. Y., Choi, Y., Stuart-Fox, D., & Huertas, B. (2021). Climate predicts both visible and near-infrared reflectance in butterflies. *Ecology Letters*, *24*(9), 1869–1879. https://doi.org/10.1111/ele.13821

Kingsolver, J. G. (1983). Ecological significance of flight activity in *Colias* butterflies: Implications for reproductive strategy and population structure. *Ecology*, *64*(3), 546–551. https://doi.org/10.2307/1939974

Kinoshita, S., & Yoshioka, S. (2005). Structural colors in nature: The role of regularity and irregularity in the structure. *ChemPhysChem*, *6*(8), 1442–1459. https://doi.org/10.1002/cphc.200500007

Krishna, A., Nie, X., Warren, A. D., Llorente-Bousquets, J. E., Briscoe, A. D., & Lee, J. (2020). Infrared optical and thermal properties of microstructures in butterfly wings. *Proceedings of the National Academy of Sciences*, *117*(3), 1566–1572. https://doi.org/10.1073/pnas.1906356117

Li, D. J., Trotta, L., Marx, H. E., Allen, J. M., Sun, M., Soltis, D. E., Soltis, P. S., Guralnick, R. P., & Baiser, B. (2019). For common community phylogenetic analyses, go ahead and use synthesis phylogenies. *Ecology*, *100*(9), e02788. https://doi.org/10.1002/ecy.2788

McKenna, D. D., Shin, S., Ahrens, D., Balke, M., Beza-Beza, C., Clarke, D. J., Donath, A., Escalona, H. E., Friedrich, F., Letsch, H., Liu, S., Maddison, D., Mayer, C., Misof, B., Murin, P. J., Niehuis, O., Peters, R. S., Podsiadlowski, L., Pohl, H., … Beutel, R. G. (2019). The evolution and genomic basis of beetle diversity. *Proceedings of the National Academy of Sciences of the United States of America*, *116*(49), 24729–24737. https://doi.org/10.1073/pnas.1909655116

Medina, I., Newton, E., Kearney, M. R., Mulder, R. A., Porter, W. P., & Stuart-Fox, D. (2018). Reflection of near-infrared light confers thermal protection in birds. *Nature Communications*, *9*(1), 3610.

Mikkola, K., & Rantala, M. J. (2010). Immune defence, a possible non-visual selective factor behind the industrial melanism of moths (Lepidoptera). *Biological Journal of the Linnean Society*, *99*(4), 831–838. https://doi.org/10.1111/j.1095-8312.2010.01398.x

Miller, E. T., Leighton, G. M., Freeman, B. G., Lees, A. C., & Ligon, R. A. (2019). Ecological and geographical overlap drive plumage evolution and mimicry in woodpeckers. *Nature Communications*, *10*, 1602. https://doi.org/10.1038/s41467-019-09721-w

Munro, J. T., Medina, I., Walker, K., Moussalli, A., Kearney, M. R., Dyer, A. G., Garcia, J., Rankin, K. J., & Stuart-Fox, D. (2019). Climate is a strong predictor of near-infrared reflectance but a poor predictor of colour in butterflies. *Proceedings of the Royal Society B: Biological Sciences*, *286*(1898), 20190234. https://doi.org/10.1098/rspb.2019.0234

Noh, M. Y., Muthukrishnan, S., Kramer, K. J., & Arakane, Y. (2016). Cuticle formation and pigmentation in beetles. *Current Opinion in Insect Science*, *17*, 1–9. https://doi.org/10.1016/j.cois.2016.05.004

Peralta-Maraver, I., & Rezende, E. L. (2021). Heat tolerance in ectotherms scales predictably with body size. *Nature Climate Change*, *11*(1), 58–63. https://doi.org/10.1038/s41558-020-00938-y

Pincebourde, S., Dillon, M. E., & Woods, H. A. (2021). Body size determines the thermal coupling between insects and plant surfaces. *Functional Ecology*, *35*(7), 1424–1436. https://doi.org/10.1111/1365-2435.13801

R Core Team. (2018). *R: A language and environment for statistical computing*. R Foundation for Statistical Computing. https://www.R-project.org/

Rabosky, D. L. (2015). No substitute for real data: A cautionary note on the use of phylogenies from birth-death polytomy resolvers for downstream comparative analyses. *Evolution*, *69*(12), 3207–3216. https://doi.org/10.1111/evo.12817

Rensch, B. (1929). *Das Prinzip geographischer Rassenkreise und das Problem der Artbildung*. Gebrueder Borntraeger.

Ross, L., Gardner, A., Hardy, N., & West, S. A. (2013). Ecology, not the genetics of sex determination, determines who helps in eusocial populations. *Current Biology*, *23*(23), 2383–2387. https://doi.org/10.1016/j.cub.2013.10.013

Schneider, C. A., Rasband, W. S., & Eliceiri, K. W. (2012). NIH image to ImageJ: 25 years of image analysis. *Nature Methods*, *9*(7), 671–675.

Seago, A. E., Brady, P., Vigneron, J. P., & Schultz, T. D. (2009). Gold bugs and beyond: A review of iridescence and structural colour mechanisms in beetles (Coleoptera). *Journal of the Royal Society Interface*, *6*, S165–S184. https://doi.org/10.1098/rsif.2008.0354.focus

Shawkey, M. D., Igic, B., Rogalla, S., Goldenberg, J., Clusella-Trullas, S., & D'Alba, L. (2017). Beyond colour: Consistent variation in near infrared and solar reflectivity in sunbirds (Nectariniidae). *Science of Nature*, *104*(9–10), 78. https://doi.org/10.1007/s00114-017-1499-8

Shi, N. N., Tsai, C. C., Camino, F., Bernard, G. D., Yu, N. F., & Wehner, R. (2015). Keeping cool: Enhanced optical reflection and radiative heat dissipation in Saharan silver ants. *Science*, *349*(6245), 298–301. https://doi.org/10.1126/science.aab3564

Stevenson, R. D. (1985a). Body size and limits to the daily range of body temperature in terrestrial ectotherms. *American Naturalist*, *125*(1), 102–117. https://doi.org/10.1086/284330

Stevenson, R. D. (1985b). The relative importance of behavioral and physiological adjustments controlling body temperature in terrestrial ectotherms. *American Naturalist*, *126*(3), 362–386. https://doi.org/10.1086/284423

Stuart-Fox, D., Newton, E., & Clusella-Trullas, S. (2017). Thermal consequences of colour and near-infrared reflectance. *Philosophical Transactions of the Royal Society B: Biological Sciences*, *372*(1724), 20160345.

Stuart-Fox, D., Rankin, K. J., Lutz, A., Elliott, A., Hugall, A. F., McLean, C. A., & Medina, I. (2021). Environmental gradients predict the ratio of environmentally acquired carotenoids to self-synthesised pteridine pigments. *Ecology Letters*, *24*(10), 2207–2218. https://doi.org/10.1111/ele.13850

Teyssier, J., Saenko, S. V., van der Marel, D., & Milinkovitch, M. C. (2015). Photonic crystals cause active colour change in chameleons. *Nature Communications*, *6*(1), 6368. https://doi.org/10.1038/ncomms7368

Thomas, G. H., Hartmann, K., Jetz, W., Joy, J. B., Mimoto, A., & Mooers, A. O. (2013). PASTIS: An R package to facilitate phylogenetic assembly with soft taxonomic inferences. *Methods in Ecology and Evolution*, *4*(11), 1011–1017. https://doi.org/10.1111/2041-210x.12117

Tian, L., & Benton, M. J. (2020a). Predicting biotic responses to future climate warming with classic ecogeographic rules. *Current Biology*, *30*(13), R744–R749.

Tian, L., & Benton, M. J. (2020b). Why climate change should generally lead to lighter coloured animals response. *Current Biology*, *30*(23), R1408.

True, J. R. (2003). Insect melanism: The molecules matter. *Trends in Ecology & Evolution*, *18*(12), 640–647. https://doi.org/10.1016/j.tree.2003.09.006

Walsberg, G. E. (1992). Quantifying radiative heat gain in animals. *American Zoologist*, *32*(2), 217–224.

Wang, L.-Y., Franklin, A. M., Black, J. R., & Stuart-Fox, D. (2021). Heating rates are more strongly influenced by near-infrared than visible reflectance in beetles. *Journal of Experimental Biology*, *224*(19), jeb242898. https://doi.org/10.1242/jeb.242898

Wilson, K., Cotter, S. C., Reeson, A. F., & Pell, J. K. (2001). Melanism and disease resistance in insects. *Ecology Letters*, *4*(6), 637–649. https://doi.org/10.1046/j.1461-0248.2001.00279.x

Wilts, B. D., Wijnen, B., Leertouwer, H. L., Steiner, U., & Stavenga, D. G. (2017). Extreme refractive index wing scale beads containing

dense pterin pigments cause the bright colors of pierid butterflies. *Advanced. Optical Materials*, *5*(3), 1600879. https://doi.org/10.1002/adom.201600879

Zwickl, D. J., & Hillis, D. M. (2002). Increased taxon sampling greatly reduces phylogenetic error. *Systematic Biology*, *51*(4), 588–598.

BIOSKETCH

Lu-Yi Wang is a PhD candidate at The University of Melbourne. Her PhD project focuses on visual and thermal adaptations to long wavelengths, including near-infrared, in jewel beetles. She also studies the biomechanics of the ultra-fast flicking movement in *Astraeus* jewel beetles.

SUPPORTING INFORMATION

Additional supporting information can be found online in the Supporting Information section at the end of this article.

How to cite this article: Wang, L.-Y., Franklin, A. M., Hugall, A. F., Medina, I., & Stuart-Fox, D. (2023). Disentangling thermal from alternative drivers of reflectance in jewel beetles: A macroecological study. *Global Ecology and Biogeography*, *32*, 408–420. https://doi.org/10.1111/geb.13632